Materials Characterization 140 (2018) 312–319

Contents lists available at ScienceDirect

Materials Characterization

journal homepage: www.elsevier.com/locate/matchar

Analysis of impact toughness scatter in simulated coarse-grained HAZ of E550 grade offshore engineering steel from the aspect of crystallographic structure

X.L. Wang[a], Z.Q. Wang[a,b], X.P. Ma[c], S.V. Subramanian[d], Z.J. Xie[a], C.J. Shang[a,e,*], X.C. Li[a]

[a] Collaborative Innovation Center of Steel Technology, University of Science and Technology Beijing, Beijing 100083, China
[b] Shougang Research Institute of Technology, Sheet Metal Research Institute, Beijing 100043, China
[c] Algoma Steel Inc., Sault Ste. Marie P6A 7B4, Canada
[d] Department of Materials Science and Engineering, McMaster University, Hamilton L8S 4L7, Canada
[e] State Key Laboratory of Metal Materials for Marine Equipment and Applications, Anshan, Liaoning 114021, China

ARTICLE INFO

Keywords:
Cooling rate
Impact toughness scatter
Crystallographic structure
Variant grouping
Crack propagation

ABSTRACT

This study aims at providing a new insights into the impact toughness scatter from the aspect of crystallographic structure. It demonstrated that the large impact toughness scatter associated much to the microstructure diversity. The crystallographic structure with evident scatter will display obvious discrepancy. In this work, three groups of samples simulated coarse-grained heat affected zone (CGHAZ) of an offshore engineering steel were obtained at different cooling rates. The Charpy test results showed that the toughness decreases dramatically with the decrease of cooling rate. However, the largest scatter in impact toughness occurred in the sample with medium cooling rate (15 °C/s), which was attributed to the heterogeneity in crystallographic structures. The visualization of crystallographic features showed that the prior austenite grain size has a significant effect on bainitic variant selection, which governed the effective grain size and crack propagation mechanism. CP (close-packed plane) grouping of variants is more likely to take place in large austenite grain, indicating that the size of CP region is larger than Bain zone, and the crack is short and flexural. On the contrary, in smaller austenite grain, Bain grouping of variants that always forms low angle grain boundary and favors crack propagation dominates the transformation, and it will promote the crack to propagate through the entire Bain zone and then yield large long crack. However, these two cases can co-exist in the same sample at medium cooling rate, indicating that the cleavage fracture is controlled by the effective grain size (Bain-zone size) and the scatter in impact toughness is associated much to the proportion and relative location between fine and coarse Bain zones.

1. Introduction

Impact toughness is an important property in engineering applications, especially for welding, whose safety is always governed by the minimum value. Generally, the large scatter in toughness can be found regularly during repeat testing, particularly in the ductile-to-brittle transition temperature (DBTT) range [1,2]. Because the microstructural variation (including different grain sizes or phases, segregated structure, or inclusion banding), mechanical issues such as the inaccuracy in notch design, temperature variation, and misalignment of the specimen during testing can all contribute to the scatter [3]. If the large scatter appears, the service safety or the grade will be reappraised according to the minimum value. Therefore, it is crucial and interested to figure out what causes scatter in toughness and what can be done to minimize it.

Considering the fracture mechanisms, the two competing fracture modes, i.e., ductile and brittle cleavage fractures, can influence both of the impact toughness and its scatter. It is generally considered that the brittle cleavage fracture is controlled by the propagation of cracks in the DBTT region [4]. Moreover, Chakrabarti et al. [4] demonstrated that increasing the microstructural heterogeneity will increase the chance of finding coarse grains at the cleavage origin, and thereby, increases the scatter in fracture toughness. Therefore, the uniformity of effective grain can be indirectly defined as the dimensions to assess the toughness scatter.

The effective grain size is difficult to be characterized from optical microscopy (OM) image but can be obtained from electron back-scattered diffraction (EBSD) image. Gourgues et al. [5,6] defined the crystallographic packet known as the Bain zone as a microstructural

* Corresponding author.
E-mail address: cjshang@ustb.edu.cn (C.J. Shang).

https://doi.org/10.1016/j.matchar.2018.03.037
Received 30 January 2018; Received in revised form 22 March 2018; Accepted 25 March 2018
Available online 27 March 2018
1044-5803/

unit and studied the crack deviation/arrest capabilities of Bain zone boundaries. Moreover, the others' studies [7,8] also indicated that high angle grain boundaries and the second phase can arrest the crack propagation. Recently, Terasaki et al. [9] clarified that the Bain zone and CP (close-packed plane) group boundaries could provide crack-propagation resistance. The Bain zone consists of ferrite variants in Kurdjumov-Sachs orientation (K—S OR) that belong to the same lattice correspondence [10,11], and the 24 variants formed in a single prior austenite grain can be divided into three Bain groups (B1: $[001]_{\gamma}//[001]_{\alpha}$, B2: $[100]_{\gamma}//[110]_{\alpha}$ and B3: $[010]_{\gamma}//[-110]_{\alpha}$). Meanwhile, the 24 variants can also be discriminated into four CP groups, each of which consists of six variants sharing the same parallel relationship of close-packed planes with austenite (CP1: $(111)_{\gamma}//(011)_{\alpha}$, CP2: $(1-11)_{\gamma}//(011)_{\alpha}$, CP3: $(-111)_{\gamma}//(011)_{\alpha}$ and CP4: $(11-1)_{\gamma}//(011)_{\alpha}$). These crystallographic features could provide a new insight into crack propagation mechanism, without which the crack propagation process will not easy to be interpreted. However, there is no further consideration on the impact toughness or its possible scatter in the previous studies. The prior austenite grain size may be uneven even in simulated samples for coarse-grained heat affected zone (CGHAZ), resulting in differential variant groups which control the size of effective grain [12].

Therefore, the present study will focus on the characterization of crystallographic structure in simulated samples of CGHAZ, including the effect of prior austenite grain size on variant selection and crack propagation. The aim is in an effort to establish a direct correlation between crystallographic structure, crack propagation and toughness scatter induced by grain heterogeneity from the aspect of crystallography.

2. Experimental

The material used in this study was an E550 grade offshore engineering steel manufactured by quenching and tempering (Q-T). As shown in Fig. 1, the microstructure of the base metal consists of tempered bainite with large amount of fine carbides dispersed in the matrix. The corresponding mechanical properties are shown in Table 1, and the chemical composition is listed in Table 2.

Gleeble-3500 thermal simulator was used to simulate single pass welding thermal cycle of CGHAZ. The samples with dimension of 60 mm × 11 mm × 11 mm (without a notch) were cut along the transverse direction of Q-T steel plate. The samples were heated to 1350 °C at a rate of 130 °C/s and held for 1 s, and then cooled at prescribed rates through the temperature range from 800 to 500 °C corresponding to $\Delta t_{8/5}$ times of 8 (fast cooling), 20 (medium cooling) and 50 (slow cooling) s. After thermal simulation, standard impact specimens with the size of 10 mm × 10 mm × 55 mm were prepared to evaluate Charpy V-Notch (CVN) impact toughness at −40 °C. Moreover, five samples were tested for the same cooling rate for repeatability so as to clear the influence of occasional factors.

Simulated CGHAZ samples for metallographic examination were sectioned at the location of the thermocouple, ensuring that the examined materials were subjected to the required thermal cycles. The samples were mechanically polished using standard metallographic procedures and etched with 4% nital for optical microscopy (OM) and scanning electron microscopy (SEM) observation. EBSD was used to study the changes of crystallographic information induced by cooling rate and the correlation between crystallographic structure and crack propagation. The samples were electropolished using the solution (glycerol:perchloric acid:alcohol = 0.5:1:8.5). EBSD data was obtained by orientation imaging microscopy (OIM) under following conditions: acceleration voltage, 20 kV; working distance, 15 mm; tilt angle, 70°; step size, 0.15 μm. Channel 5 software from Oxford-HKL was employed for post-processing orientation data. Matlab software was used for calculating theoretical pole figures and variant fraction in different austenite grains.

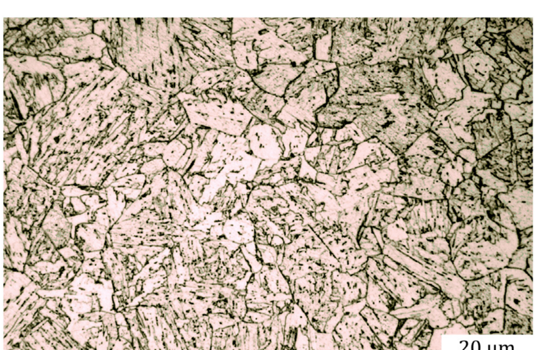

Fig. 1. Optical micrograph showing the microstructure of base metal.

Table 1
Mechanical properties of base metal.

Steel	Status	Thickness (mm)	Yield strength (MPa)	Tensile strength (MPa)	Total elongation (%)	−40 °C impact energy (J)
E550	Q-T	36	554	707	21	152 ± 15

Table 2
Chemical composition of base metal (wt%).

C	Si	Mn	Ni	Nb	Cr	Mo	Cu	Ti	P	S
0.063	0.26	1.38	0.65	0.044	0.40	0.22	0.35	0.017	0.0081	0.0016

3. Results and Discussion

3.1. Charpy Impact Toughness

The results of Charpy impact toughness performed at −40 °C of the simulated CGHAZ with different cooling rates are given in Fig. 2. As the cooling rate decreases, the average impact energy declines dramatically from 170 to 27 J. Similar tendency can be found in the single minimum. Single minimum represents the lowest toughness that was measured and should be very important from the engineering aspect [13]. The lowest Charpy values caused by low toughness zones, would dominate the fracture behavior of the entire weldment. Therefore, the average impact energy and single minimum are both presented in Fig. 2. It can

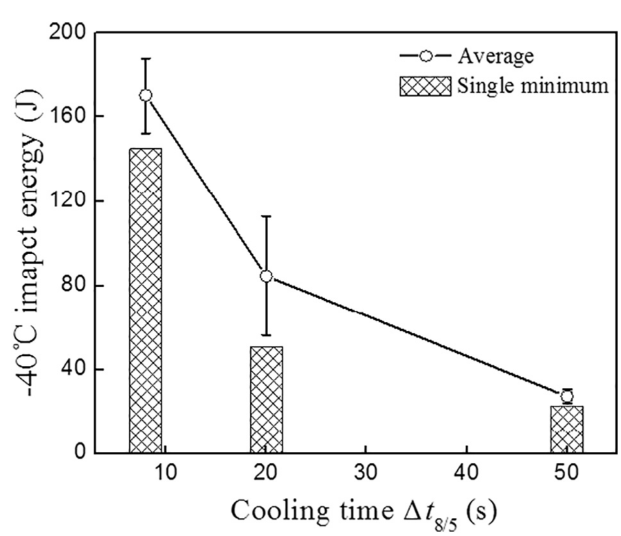

Fig. 2. Charpy impact toughness of simulated samples.